



CRUSTAL CARBONATITES: DEFINITION, GEOLOGY, MINERALOGY, AND GEOCHEMISTRY

E.V. Sklyarov ¹✉, A.V. Lavrenchuk ^{2,3}

¹ Institute of the Earth's Crust, Siberian Branch of the Russian Academy of Sciences, 128 Lermontov St, Irkutsk 664033, Russia

² Sobolev Institute of Geology and Mineralogy, Siberian Branch of the Russian Academy of Sciences, 3 Academician Koptug Ave, Novosibirsk 630090, Russia

³ Novosibirsk State University, 1 Pirogov St, Novosibirsk 630090, Russia

ABSTRACT. This is a synopsis of the available data on crustal carbonatites, including their temporal and spatial distribution, mineralogy, geochemistry, and stable isotope ($\delta^{18}\text{O}$ and $\delta^{13}\text{C}$) patterns. Crustal carbonatites are intrusive rocks containing >50 vol. % carbonate minerals and ≤ 20 wt. % SiO_2 , which crystallize from partial melts of primary sedimentary carbonate rocks in the lower crust. They commonly occur as dykes in high-grade metamorphic complexes, bear silicate minerals typical of metasomatic environments, show isotopic and geochemical signatures of carbonate sediments or transitional varieties to mantle-derived carbonatites, and are emplaced during tectonic activity in strike-slip, rifting, or postcollisional extension settings. Partial melting of carbonate material in the crust and intrusion of melt batches to shallower crust levels is possible provided that primary carbonate sediments are present in the lower crust while the melting region is heated up by underplated mantle mafic magma and is fluxed sufficiently with H_2O -rich fluids.

KEYWORDS: crustal carbonatite; dyke; mineralogy; geochemistry; Olkhon terrane; West Baikal area

FUNDING: The work was carried out as part of government assignments to the Institute of the Earth's Crust, Irkutsk, and to the Sobolev Institute of Geology and Mineralogy, Novosibirsk (Project 122041400044-2).



EDN: ZDTBEN

REVIEW

Correspondence: Eugene V. Sklyarov, skl@crust.irk.ru

Received: December 17, 2024

Revised: January 9, 2025

Accepted: January 13, 2025

FOR CITATION: Sklyarov E.V., Lavrenchuk A.V., 2025. Crustal Carbonatites: Definition, Geology, Mineralogy, and Geochemistry. *Geodynamics & Tectonophysics* 16 (1), 0805. doi:10.5800/GT-2025-16-1-0805

1. INTRODUCTION

Carbonatites are intrusive or extrusive igneous rocks defined by mineralogic composition consisting of greater than 50 % carbonate minerals and no more than 20 wt. % SiO_2 [Le Maitre, 2002]. These rocks, with their particular mineralogy and chemistry, have been a focus of attention also due to their significant economic potential as hosts of world-class deposits of REE, rare metals, alkaline earth metals, iron, and non-metallic resources. They are assumed to be of mantle origin associated with high-temperature melting of carbonate material [Bell, Tilton, 2002; Wyllie, Tuttle, 1960].

The term "carbonatite" was traditionally applied to rocks originated in the mantle, with the respective chemical and mineralogical specificity, before evidence of intrusive carbonate rocks with crustal composition fingerprints appeared in the early 2000s [Lentz, 1999; Liu et al., 2006; Roberts, Zwaan, 2007; Wan et al., 2008; Sklyarov et al., 2009, 2013, 2022; Dolenec et al., 2015; Wu et al., 2022; Wickramasinghe et al., 2024; etc.]. Such rocks were termed in different ways distinctive from the classical mantle-derived carbonatites: carbonatite-like dyke [Liu et al., 2006; Dolenec et al., 2015], emanating marble dyke [Roberts, Zwaan, 2007], crustal carbonatite [Wan et al., 2008], pseudo-carbonatite [Sklyarov et al., 2009], culdimite carbonatite

[Proskurnin et al., 2010], injection marble and calciphyre [Sklyarov et al., 2013], marble dyke [Sklyarov et al., 2022], para-carbonatite [Su et al., 2024a], or even pegmatitic carbonate rock [Su et al., 2024b]. The term crustal carbonatite coined by [Wan et al., 2008] and used in recent publications e.g. [Jin et al., 2024a] appears the most appropriate. We argue that this term is rightful though some authors doubted it. For instance [Mitchell, 2005, p. 2063] wrote "A third group of carbonate-rich rocks formed by pneumatolytic melting of crustal rocks should not even be considered as carbonatites (*sensu lato* or *stricto*)". This paper presents a summary of the available mineralogical, geochemical, and isotopic data on crustal-derived carbonatites.

2. GEOLOGY AND OCCURRENCE PATTERNS OF CRUSTAL CARBONATITES

Currently, more than 600 occurrences of mantle-derived carbonatites are known from all continents except Antarctica, as well as from oceanic settings [Humphreys-Williams, Zahirovic, 2021], while the known crustal carbonatite sites are almost 100 times fewer. Most of them are located in Eurasia (Fig. 1) and a few were found in North and South America. In almost all cases, crustal carbonatites exist within amphibolite- to ultrahigh-temperature granulite facies metamorphic complexes, or sometimes in related

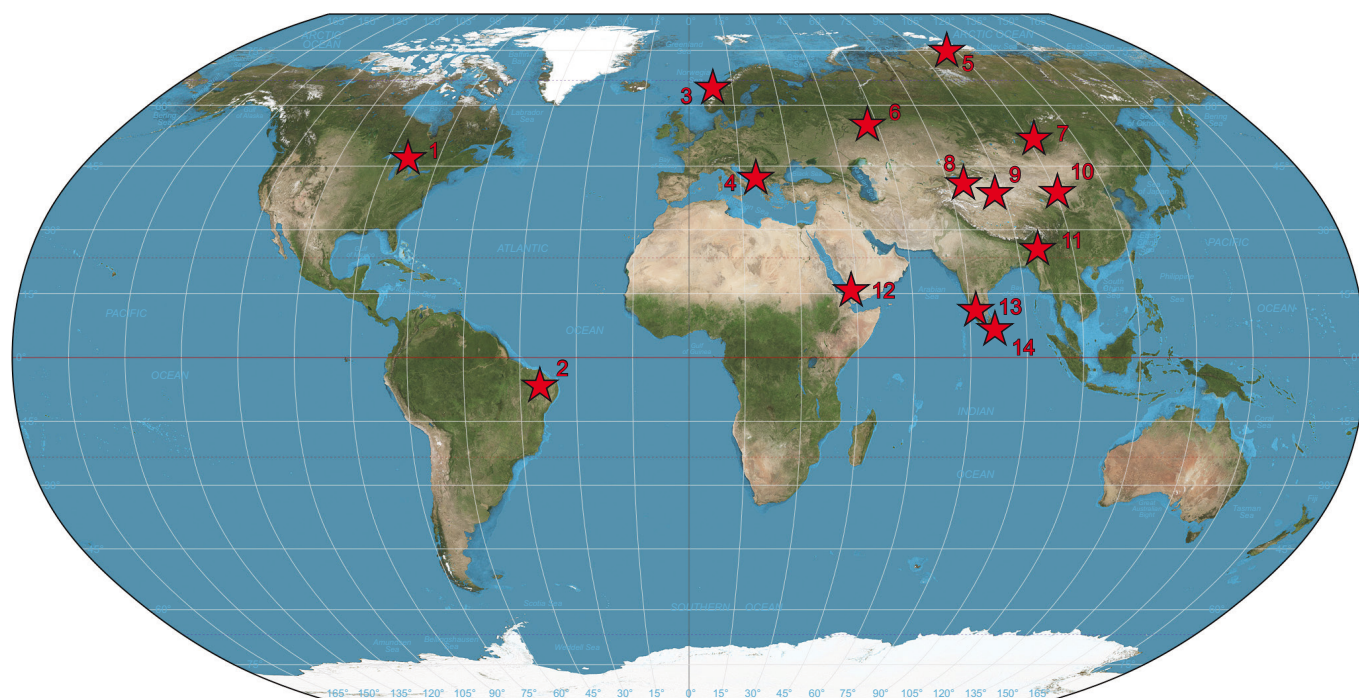


Fig. 1. Global distribution of crustal carbonatites.

1 – south-western Grenville Province, Canada, Mesoproterozoic [Lentz, 1998]; 2 – north-eastern Brazilian craton, Brazil, Paleoproterozoic [Santos et al., 2013]; 3 – orogenic complex in Norway, Early Paleozoic [Roberts, Zwaan, 2007]; 4 – Madenska River complex, Macedonia, Mesozoic [Dolenec et al., 2015]; 5 – Taimyr Peninsula, Mesozoic [Proskurnin et al., 2010]; 6 – Khabarny pluton, Ural Mountains, Russia, Paleozoic [Fershtater, Pushkarev, 1988]; 7 – Olkhon metamorphic terrane, West Baikal area, Russia, Early Paleozoic [Sklyarov et al., 2009, 2013, 2022]; 8 – north-western Tarim craton, China, Late Paleozoic [Jin et al., 2024a]; 9 – south-eastern Tarim craton, China, Paleoproterozoic [Yang et al., 2012; Wu et al., 2022]; 10 – northern margin of North China craton, China, Paleoproterozoic [Wan et al., 2008]; 11 – Himalayan syntaxis, China, Neogene [Liu et al., 2006]; 12 – Al-Mahfid gneiss terrane, Yemen, Neoproterozoic [Le Bas et al., 2004]; 13 – southern Indian craton, India, Mesoproterozoic [Hegner et al., 2020]; 14 – Highland complex, Sri Lanka, Neoproterozoic [Wickramasinghe et al., 2024].

intrusions [Liu et al., 2006; Wan et al., 2008; Sklyarov et al., 2022; Wickramasinghe et al., 2024; etc.].

The known crustal carbonatite dykes vary in age from Paleoproterozoic to Neogene. The oldest dykes occur in Precambrian cratons, such as Paleoproterozoic carbonatites in the Brazilian [Santos et al., 2013], Tarim [Yang et al., 2012; Wu et al., 2022], and North China [Wan et al., 2008] cratons and Mesoproterozoic carbonatites in the southern Indian craton [Hegner et al., 2020]. Younger occurrences of carbonatites are Neoproterozoic in a gneissic terrane in Yemen [Le Bas et al., 2004] and Early Paleozoic in the Olkhon metamorphic terrane [Sklyarov et al., 2022], an orogenic area in Norway [Roberts, Zwaan, 2007], and in the margin of the Indian craton [Wickramasinghe et al., 2024]. Mesozoic carbonatites were reported from the Sri Lanka Precambrian UHT metamorphic complex [Wickramasinghe et al., 2024] and the Madenska River complex in Macedonia [Dolenec et al., 2015]. Neogene carbonatite dykes were found in the Himalayan Syntaxis, western Himalayas [Liu et al., 2006].

Carbonatitic igneous bodies can be emplaced in different ways but are especially well distinctive as dykes hosted by metamorphic complexes [Liu et al., 2006; Roberts, Zwaan, 2007; Wan et al., 2008; Sklyarov et al., 2013, 2022; Wu et al., 2022; Wickramasinghe et al., 2024], as well as by gabbro and syenite [Sklyarov et al., 2013, 2022] or ultramafic [Fershtater, Pushkarev, 1988] intrusions. The dykes are from few centimeters to tens of meters thick and are either sporadic [Roberts, Zwaan, 2007; Sklyarov et al., 2022; Su et al., 2024b] or cluster in swarms comprising hundreds of bodies within relatively small areas [Liu et al., 2006].

In the Olkhon terrane, carbonatite dykes are rare and are reliably identified mainly in coastal cliffs of Lake Baikal (Fig. 2). A few 0.3 m to 3 m thick dykes crosscut amphibolites and can be misinterpreted as layers in the carbonate-section being poorly exposed and oriented oblique to the amphibolite schistosity (Fig. 2, D, E). The dykes have 3–10 cm thick white margins around a dark gray core

(Fig. 3). The dark gray color is produced by disseminated graphite tracing calcite grain boundaries, which is much more abundant than the sporadic graphite flakes in the margins. Many dykes have intricate shapes due to their origin in strike-slip settings (Fig. 4). Carbonatite dykes in several occurrences coexist with dolerite (metadolerite) dykes (see Fig. 3).

In addition to amphibolites, the dykes occur also in the 500 Ma Birkhin gabbro and 460 Ma Ust'-Krestovsky subalkaline gabbro (Fig. 5) complexes, with a large dyke swarm on the periphery of the latter (see Fig. 2, B). It consists of about twenty 0.3 to 3 m thick dykes of calcitic carbonatites, mostly with low percentages of silicate minerals ($\leq 5\%$) except for few dykes which bear xenoliths with compositionally variable typically skarn mineral assemblages.

Some more dykes are emplaced in two intrusions of the Birkhin gabbro complex in the Buguldeika intrusion (see Fig. 2, A), where a gently dipping ≤ 2 m thick dyke of dolomite-calcite carbonatite (Fig. 6, a) is traceable for 150 m. The Buguldeika carbonatite is pinkish white, fine-grained and almost free from silicate minerals; the dyke margins bear up to 0.1 m thick skarn lenses (Fig. 6, b) of pyroxene-zoisite-plagioclase or garnet-pyroxene mineralogy.

Dolerite and carbonatite dykes (Fig. 7) cluster in a 150 m wide and more than 1 km long zone in the southern margin of the Birkhin intrusion (see Fig. 2, C). The dolerite bodies enclose small skarn lenses formed under high (melilite and wollastonite) or moderate (garnet and pyroxene) temperatures. We mapped at least ten carbonatite dykes, from 0.5 to 45 m thick and 50 to 150 m long. Judging by the relative position of the dykes, carbonatitic and doleritic magma intruded almost synchronously in small batches during tectonic activity.

Less often carbonatite bodies appear within complexly structured intrusions, e.g., a 100 m thick body traceable discontinuously for >700 m in dolomitic-calcic carbonatite coexisting with pyroxenite and nepheline-pyroxene rocks (Fig. 8) in the central part of the Tazheran gabbro-syenite

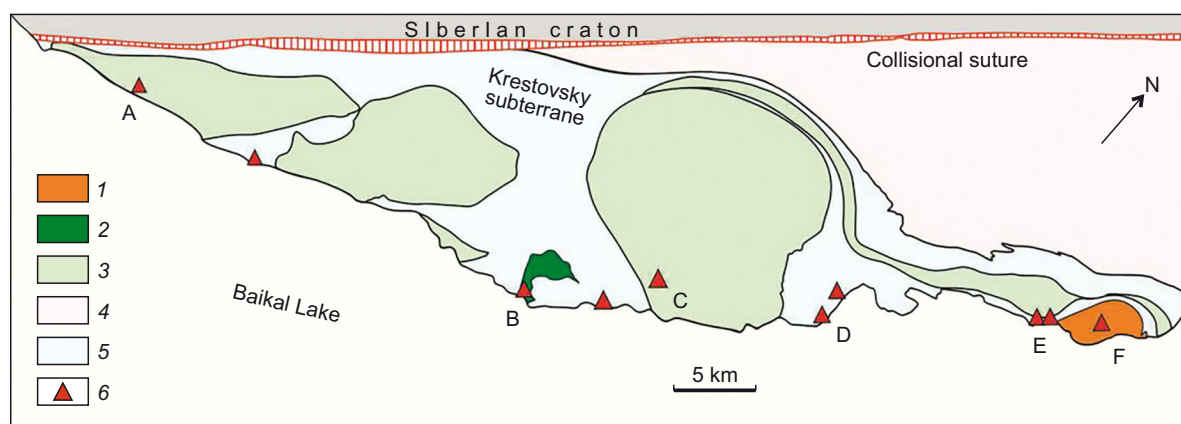


Fig. 2. Crustal carbonatite dykes in several complexes of the Olkhon terrane.

1 – Tazheran gabbro-syenite; 2 – Ust'-Krestovsky subalkaline gabbro complex (460 Ma); 3 – Birkhin gabbro complex (500 Ma); 4 – predominantly marble-gneiss metamorphic complex; 5 – marble-amphibolite metamorphic complex; 6 – letters mark occurrences discussed in the paper: Buguldeika intrusion (A), Ust-Krestovsky intrusion (B), Birkhin intrusion (C), amphibolite in the mouth of the Anga River (D), amphibolite near Tazheran complex (E) and within the latter (F).



Fig. 3. Carbonatite dyke in amphibolite derived from Begul gabbro (a) and its enlarged fragment (b), Olkhon terrane, after [Sklyarov et al., 2022].

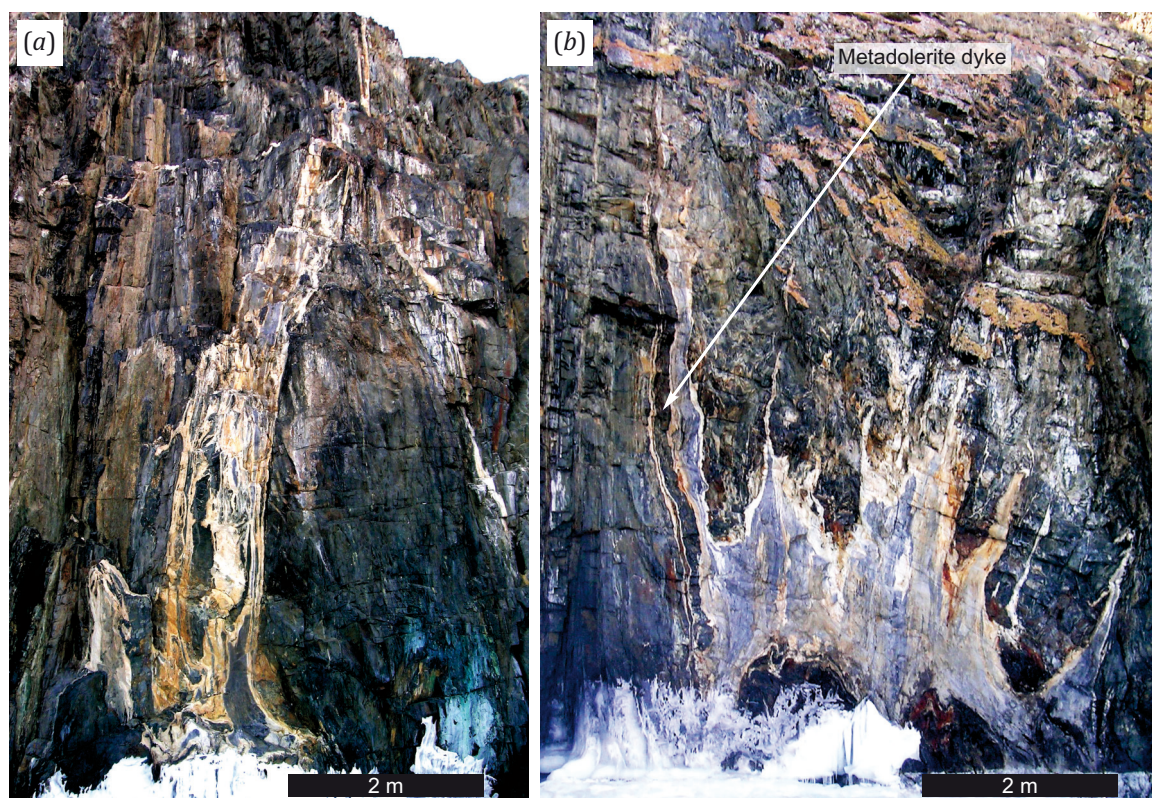


Fig. 4. Complexly structured dykes of calcitic carbonatite in amphibolite derived from Begul gabbro, after [Sklyarov et al., 2022]. (a) – mottled dyke; (b) – deformed dyke next to a metadolerite dyke.

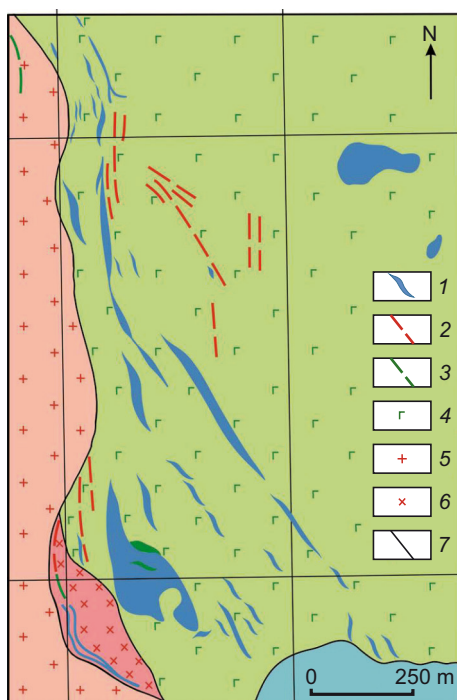


Fig. 5. Crustal carbonatite dykes in Ust-Krestovsky gabbro, (after [Sklyarov et al., 2021]). 1 – carbonatite dykes; 2 – granite veins; 3 – dolerite dykes; 4 – subalkaline gabbro of the Ust-Krestovsky complex (460 Ma); 5 – granite; 6 – diorite; 7 – geological boundaries.

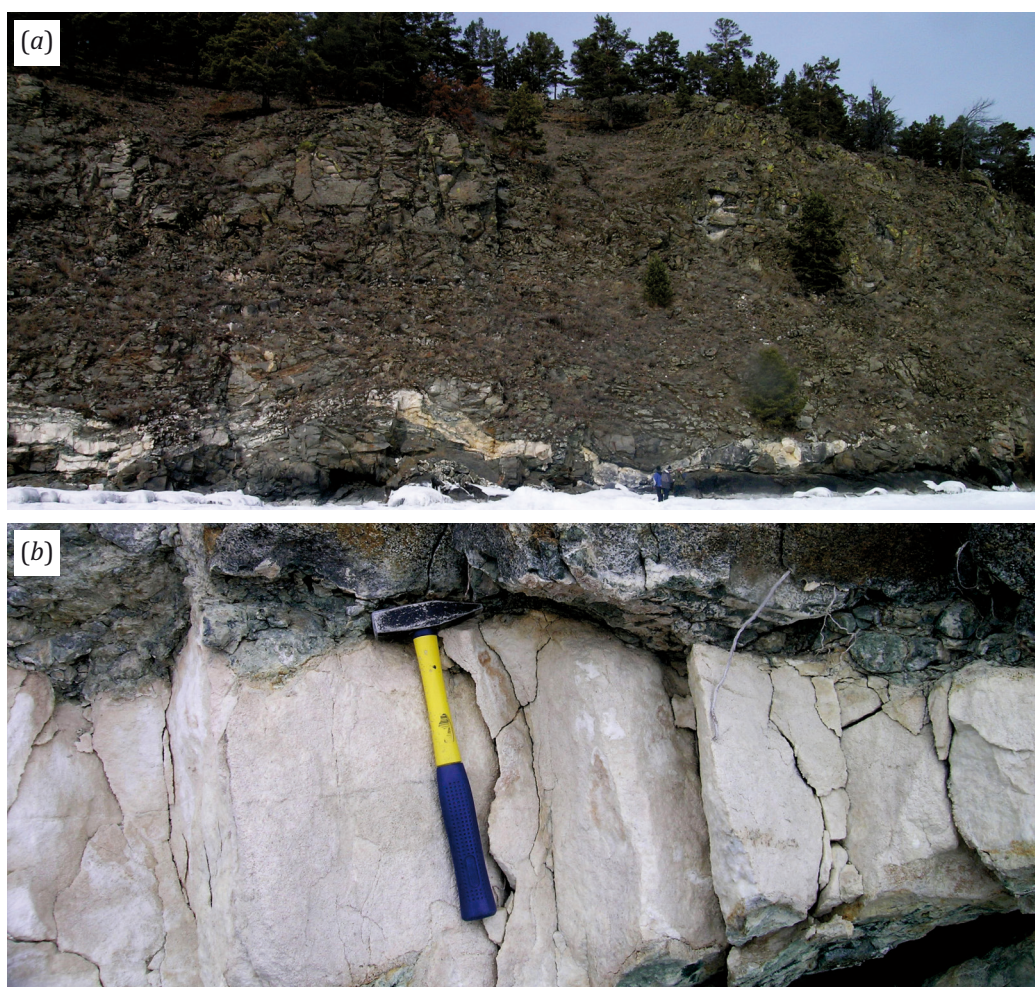


Fig. 6. Gently dipping carbonatite dyke in Buguldeika intrusion (a) and its enlarged fragment with skarn lenses along the margins (b).

complex (see Fig. 2, F). It consists of medium-grained to ultra-coarse rocks, locally with few centimeters to few tens of meters angular fragments of more or less abundant skarn after fassaitic pyroxenite (Fig. 9). The pyroxenite likely crystallized from a mafic melt contaminated with carbonate material, while the carbonate and mafic melts were emplaced almost synchronously.

Crustal carbonatites are remarkable by enclosing xenoliths of more or less abundant skarn after silicate rocks, most often fragments of mafic [Le Bas et al., 2004; Wickramasinghe et al., 2024; etc.] or ultramafic [Fershtater, Pushkarev, 1988] host metamorphics. Such fragments vary in size from a few meters [Wickramasinghe et al., 2024] to tens of centimeter or a few centimeters [Liu et al., 2006; Le Bas et al., 2004;

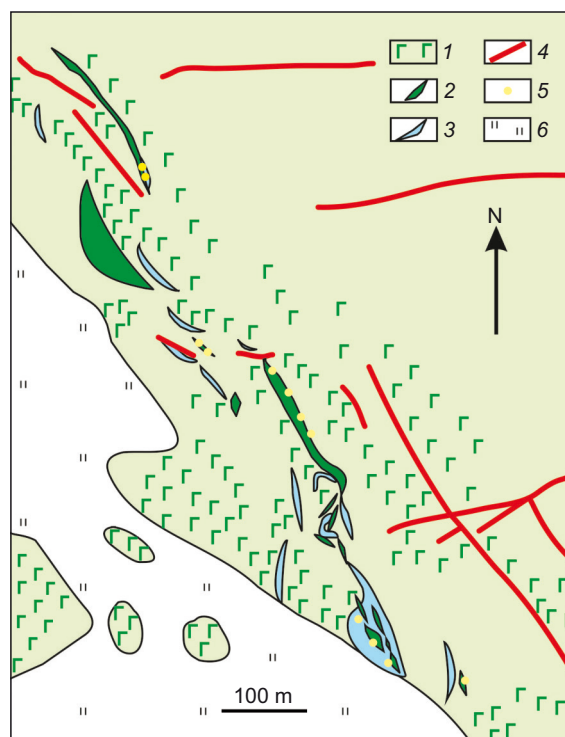


Fig. 7. Detailed geological map of the southern Birkhin intrusion (see Fig. 2, B) (after [Sklyarov et al., 2020]).

1 – Birkhin gabbro (500 Ma); 2 – dolerite and beerbachite; 3 – crustal carbonatite dykes; 4 – aplitic and granitic veins; 5 – anti-skarn of garnet-clinopyroxene-wollastonite or more rarely melilite-garnet-pyroxene-wollastonite mineralogy; 6 – lacustrine-alluvial sediments.

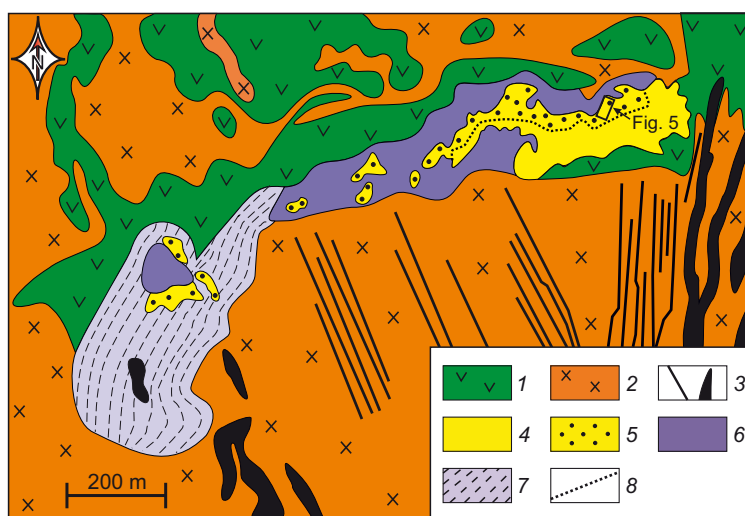


Fig. 8. Central part of Tazheran massif: a geological map (after [Sklyarov et al., 2021]).

1 – beerbachite after tholeiitic dolerite and gabbro; 2 – syenite; 3 – subalkaline gabbro and microgabbro; 4–5 – dolomitic-calcic marble (4) with pyroxenite fragments (5); 6 – pyroxenite and nepheline-pyroxene rocks; 7 – metasomatic Grt-Mll-Cpx and Mll-Woll zone; 8 – boundary between "pure" marble and marble containing pyroxenite fragments. Mineral names are abbreviated as in [Warr, 2021].

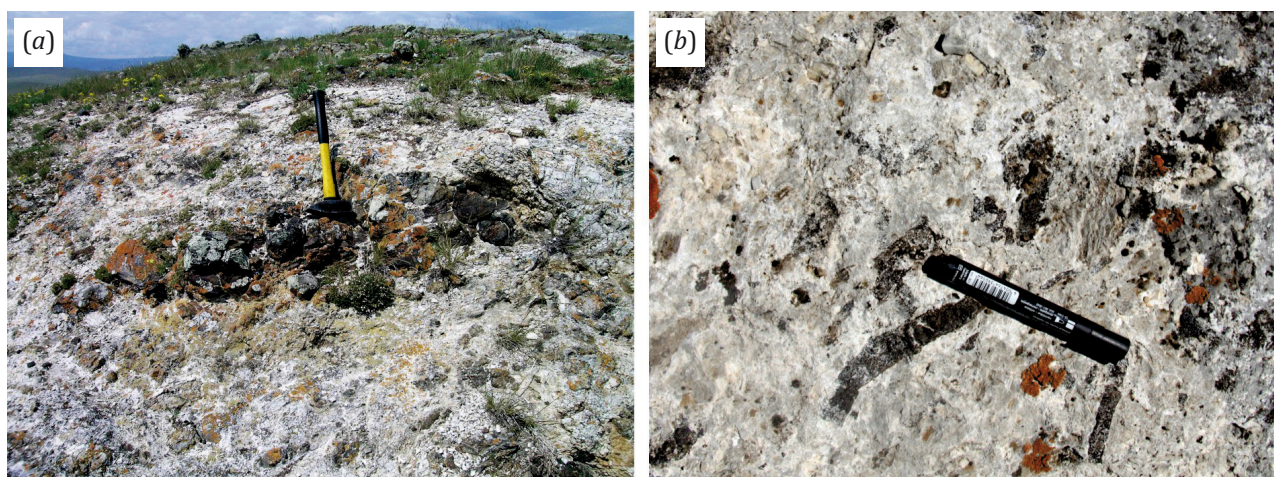


Fig. 9. Pyroxenite fragments in crustal carbonatite. (a) – skarn after pyroxenite in coarse-grained carbonatite; (b) – small angular fragments of skarn after pyroxenite in coarse-grained carbonatite.

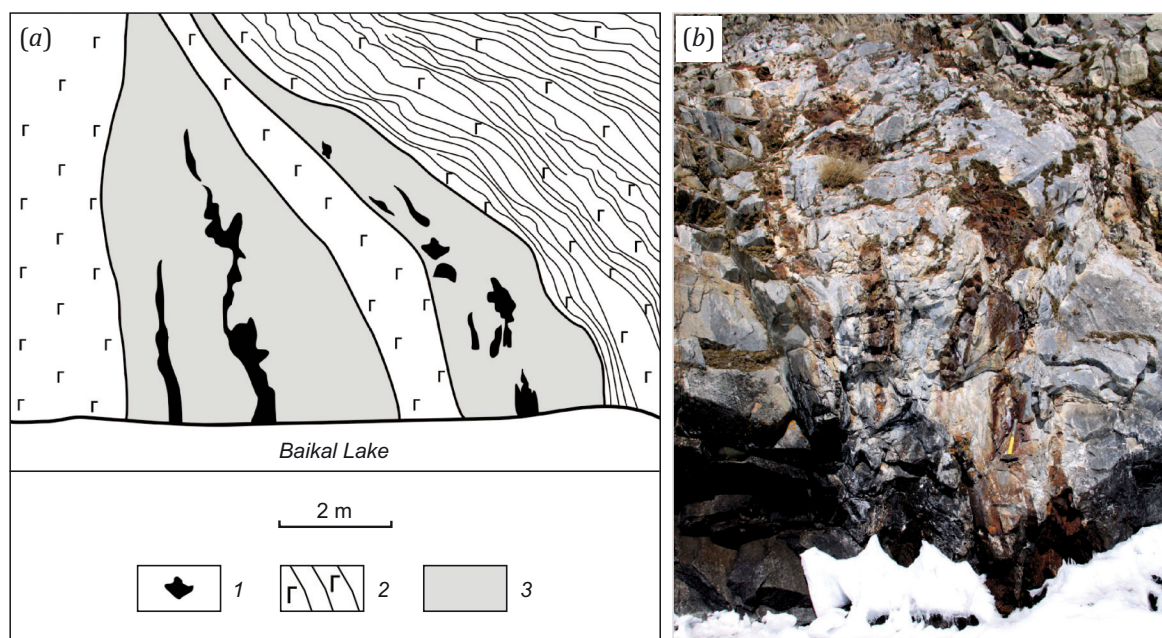


Fig. 10. Sketch of two carbonatite dykes and dismembered pyroxene porphyrite dykes in their interior (a) and photograph of the lower part of the dismembered dyke on the right (after [Sklyarov et al., 2022]) (b). 1 – pyroxene porphyrite; 2 – host subalkaline Ust-Krestovsky gabbro; 3 – crustal carbonatite.

Wan et al., 2008; Santos et al., 2013; Dolenec et al., 2015; etc.]. The compositionally different fragments apparently traveled kilometers from the place where they were captured by the carbonate melt, which is consistent with the absence of the respective lithologies from the dyke sites, e.g., dunite fragments in carbonatite dykes in the Khabarny clinopyroxenitic intrusion in the Urals and high-Cr chromite (typical of dunite) in the carbonatite component [Fershtater, Pushkarev, 1988].

However, some xenoliths represent mafic dykes emplaced together with carbonatitic magma rather than being wall rock fragments it entrapped. This is the case of dismembered dykes in the interior of two carbonatite dykes within the Ust'-Krestovsky gabbro (Fig. 10) which are com-

posed of pyroxene markedly different from the host gabbro in structure and chemistry. The mafic melt crystallized earlier, and the porphyritic dyke was brecciated and dispersed by the carbonatitic melt. On the other hand, it is obvious that the carbonate and mafic melts were emplaced simultaneously. Dolerite dykes are often proximal and quasi-parallel to carbonatite dykes; sometimes they become dismembered during tectonic movements (see Fig. 3) and acquire intricate shapes as a result of synmetamorphic deformation (see Fig. 4).

3. MINERALOGY OF CRUSTAL CARBONATITES

Carbonatite dykes are most often calcitic and less often dolomitic [Liu et al., 2006; Wan et al., 2008; Le Bas et

al., 2004], or have mixed dolomite-calcite [Sklyarov et al., 2013, 2022] compositions. The mineralogy also includes 2–3 to 50 % of silicate and oxide phases, as well as minerals of other groups. The mineralogical patterns are controlled by the type of carbonates. Non-carbonate phases in dolomitic and dolomitic-calcic carbonatites are mainly forsterite, phlogopite, spinel, and diverse accessories. For instance, dolomitic carbonatites from the Himalayan Syntaxis contain accessory astrophyllite, apatite, zircon, garnet, pargasite, geikielite-ilmenite, varvikite, pyrite-pyrrhotite, and celestine-barite [Liu et al., 2006]. The known accessories in dykes from the North China craton include plagioclase, quartz, clinopyroxene, phlogopite, garnet, amphibole, and zircon [Wan et al., 2008]. The Tazheran carbonatites bear clinohumite, besides forsterite and spinel, as well as accessory perovskite, calzirtite, tazheranite, geikielite, Mg-ilmenite, apatite, and magnesioferrite.

The mineralogy of calcic carbonatites is ever more diverse, and mineral assemblages in different dykes can differ even within same localities. Main phases are diopside-hedenbergite pyroxenes, amphibole, wollastonite, grossular-andradite garnets, epidote-clinzoisite, allanite, scapolite, phlogopite, forsterite, K-feldspar, quartz, and graphite, while the accessories are iron oxides, apatite, titanite, ilmenite, zircon, or rarely REE phases. Crustal carbonatites, with their typical skarn minerals, are often erroneously attributed to felsic or mafic igneous bodies (see below).

4. GEOCHEMISTRY AND STABLE ISOTOPES

The trace-element chemistry of crustal carbonatites depends mainly on carbonate minerals (calcite or dolomite, or less often both) and on the total percentage of

silicates. Unlike their mantle-derived counterparts, crustal carbonatites have low contents of indicator trace elements, especially REEs. The signatures of crustal carbonatites poor in silicates are similar to those of carbonate sediments, whereas the varieties with larger percentages of silicate phases contain trace elements in higher concentrations, though lower than in the mantle-derived carbonatites. Trace-element contents in carbonatites from the Olkhon terrane are mostly intermediate between the values of mantle carbonatites and sedimentary carbonate rocks. However, it is hard to trace any distinct geochemical trends because of high variability in element contents, even within same bodies.

Among isotopic signatures, oxygen ($\delta^{18}\text{O}$) and carbon ($\delta^{13}\text{C}$) isotope compositions are the most informative. The isotopic ratios of crustal carbonatites are most often intermediate between mantle-derived carbonatites and carbonate sediments ($\delta^{18}\text{O}_{\text{PDB}} = 11 \dots +19$; $\delta^{13}\text{C}_{\text{SMOW}} = -5.5 \dots +8$) or are similar to the latter in a few cases [Liu et al., 2006; Wan et al., 2008; Dolenec et al., 2015; Doroshkevich et al., 2017; Hegner et al., 2020; Wickramasinghe et al., 2024]. Perfect match to carbonate sediment was reported for carbonatites from the Himalayan Syntaxis and some carbonatites in the Tazheran complex of the Olkhon terrane (Fig. 11). The Tazheran carbonatites and marbles have identical $\delta^{18}\text{O}_{\text{PDB}}$ but the $\delta^{13}\text{C}_{\text{SMOW}}$ values are lighter in carbonatites.

5. CONDITIONS FOR THE FORMATION OF CRUSTAL CARBONATITES

As it was shown experimentally long ago [Wyllie, Tuttle, 1960], melting of carbonate material requires high temperatures above 1300 °C. Therefore, carbonatitic melts

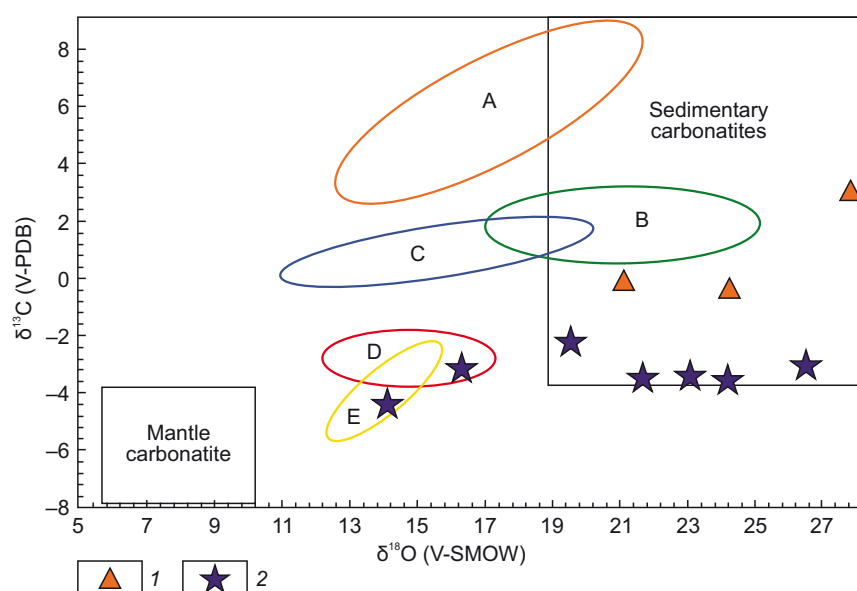


Fig. 11. $\delta^{13}\text{C}$ vs $\delta^{18}\text{O}$ diagram for crustal carbonatites of the Olkhon terrane.

1 – metamorphic dolomite and calcite marbles of the Olkhon terrane; 2 – crustal carbonatites of the Olkhon terrane, after [Doroshkevich et al., 2017]. Fields A to E refer to crustal carbonatites from other areas: A – Brazilian craton, after [Santos et al., 2013], B – Himalayan syntaxis, after [Liu et al., 2006], C – Madenska River complex, Macedonia, after [Dolenec et al., 2015], D – UHT granulite-facies metamorphic terrane of Sri Lanka, after [Wickramasinghe et al., 2024], E – North China craton, after [Wan et al., 2008]. Primary igneous carbonatites (box) and carbonate sediments are after [Bell, 2005; Keller, Hoefs, 1995].

were considered to originate uniquely in the mantle, by different mechanisms: (1) partial melting of carbonate-bearing peridotite or eclogite e.g., [Yaxley, Brey, 2004]; (2) separation of immiscible carbonatite magma from silica-undersaturated carbonate melts [Brooker, Kjarsgaard, 2011]; (3) evolution of silica-undersaturated alkaline and carbonate melts with formation of a residual melt [Watkinson, Wyllie, 1971]. Meanwhile, the experimental result showing calcite to melt at 700 °C in water-bearing systems [Wyllie, Tuttle, 1960] remained overlooked. Later a similar effect, with further temperature decrease to 600 °C, was observed in experiments with added MgO [Fanelli et al., 1986]. The process is, however, limited by a narrow range of relative CO₂ and H₂O contents required to decrease the melting temperature. Recent experiments confirmed that melting of calcite can start at 650 °C [Durand et al., 2015; Floess et al., 2015]. This important empirical evidence undermines the idea that carbonatitic magma generation is only possible at the mantle depths and makes expecting that melting of primary carbonate sediments in the lower crust may be as widespread as the formation of granitic melts. The rare occurrence of crustal carbonatites is likely due to several reasons: (i) the fluid involved in melting should be rich in H₂O and poor in CO₂; (ii) sedimentary carbonate material is less abundant in the lower crust than silicate rocks; (iii) any unusual occurrences of carbonate rocks found in poorly exposed terrains are commonly interpreted as

marble layers or xenoliths, or protrusions, or hydrothermal veins.

The possibility for melting of primary sedimentary carbonates was surprisingly supported by recent data from volcanic and plutonic complexes [Barnes et al., 2005; Iacono Marziano et al., 2008; Mollo et al., 2010; Gaeta et al., 2009; Ganino et al., 2013; Carter, Dasgupta, 2016; etc.]. Namely, isotope geochemical and mineralogical signatures, as well as experimental evidence, revealed carbonate assimilation by silicate magma. The assimilated carbonate material was apparently liquid and existed as carbonate-rich partial melts rather than solid xenoliths or wall rock fragments. The assimilation biased the isotope-geochemical signatures of silicate melts and produced minerals uncommon to igneous lithologies, such as fassaite (high-Al calcic pyroxene) typical of high-temperature metasomatic rocks. Unusual fassaitic and nepheline-fassaitic pyroxenites [Sklyarov et al., 2021], as well as fassaitic gabbro [Sklyarov et al., 2024], which presumably crystallized from a contaminated mafic melt, were found in the Olkhon terrane. Data from volcanic complexes have provided convincing evidence that carbonate melting in the crust is a common process.

Crustal carbonatitic melts can form in skarn-producing systems upon interaction with syenite magma, as it was suggested proceeding from empirical evidence on low-temperature melting of limestone [Lentz, 1999] (Fig. 12). According to the model of [Lentz, 1999], skarn forms above

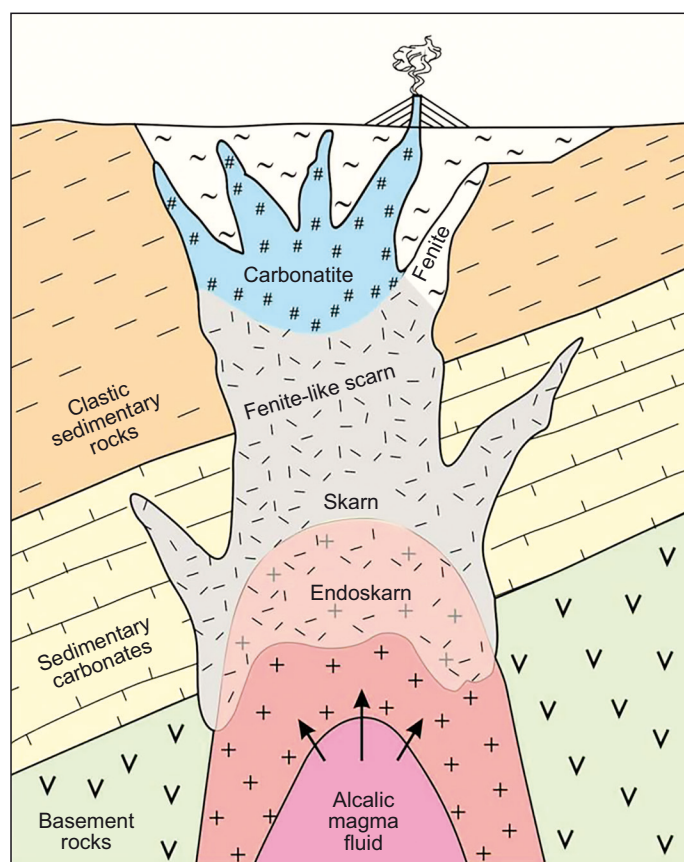


Fig. 12. A sketch of hypothetical intrusion-limestone interaction producing skarn, fenite-like skarn, fenite, and "distal" carbonatitic magma in the upper crust via simple volatile fluxing, after [Lentz, 1999].

an intrusion interacting with limestone, under the effect of magma-derived fluids (volatile fluxing), simultaneously with some amount of carbonatitic magma emplaced at the upper crustal levels. Thus, crustal carbonatite can form provided that the crust at lower or intermediate depth levels contains sedimentary carbonate material while syenite magma is saturated with volatiles. In this respect, relatively large plutons can be expected to occur beneath the known crustal carbonatite occurrences. The formation together with skarn can account for the typical skarn mineral assemblages of crustal carbonatites, as they can be entrapped in the carbonate melting zone.

Meanwhile, besides being transported from zones of silicate magma-carbonate interaction, metasomatic silicate minerals and their aggregates can originate at the contact of carbonatite dykes with silicate rocks, but by a mechanism different from the classical skarn formation. The diverse skarn metasomatic mineral assemblages form

when fluids derived from cooling silicate magma react with carbonate wall rock material [Korzhinskii, 1970; Meinert, 1992]. In the case of carbonatites, on the contrary, it is the effect of hydrous carbonate melts on silicate wall rocks that produces skarn along the contact, as it was observed in some dykes from the Olkhon terrane (see Fig. 6, b). Therefore, interaction of two compositionally contrasting components in the presence of an aqueous fluid leads to the same result in both cases. To make distinction from the classical skarn, Anenburg [Anenburg, Mavrogenes, 2018; Anenburg, Walters, 2024] coined the term "antiskarn" for that associated with carbonatites. Finally, metasomatic minerals in crustal carbonatites can crystallize directly from a melt (which is colder than the parental melt of mantle-related carbonatites) and/or precipitate as secondary minerals replacing the primary magmatic assemblages during slow cooling of carbonatitic magma under continuing flux of H_2O-CO_2 fluids. The latter mechanism

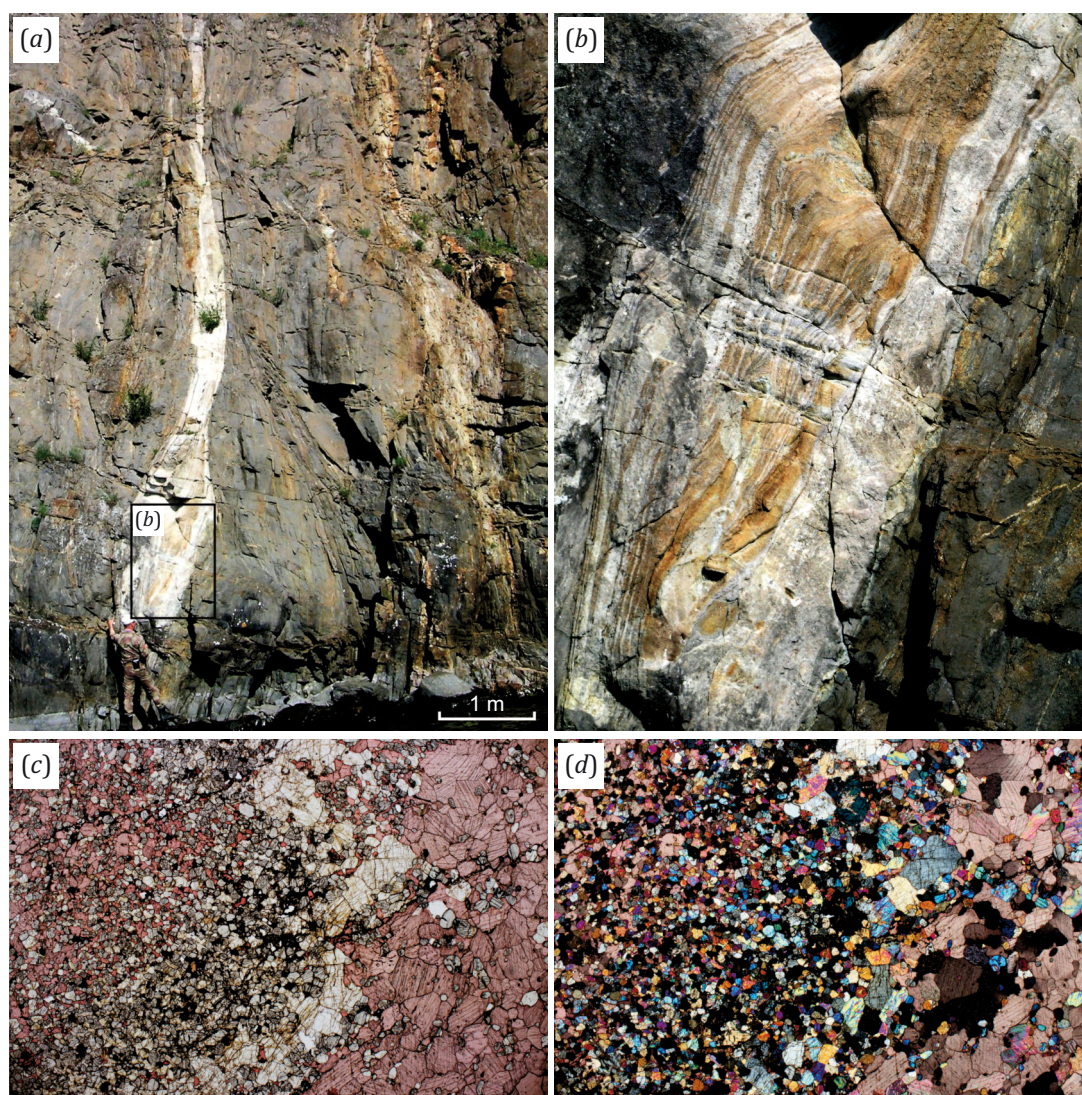


Fig. 13. Dyke of crustal calcic carbonatite with a silicocarbonatite "core".

(a) – general view; (b) – enlarged dyke fragment; (c, d) – microphotographs of the carbonatite-silicocarbonatite contact, in plane polarized (c) and cross polarized (d) light. Field size 9.0×5.8 mm. Mineral assemblage: calcite, clinopyroxene, phlogopite, scapolite, K-feldspar, titanite, metallic phase.

was invoked to explain the origin of metasomatic silicate minerals in the Alnö mantle-derived carbonatites, Sweden [Vuorinen, Skelton, 2004].

The crystallization of skarn minerals from a melt is illustrated by a carbonatite dyke (see Fig. 2, E) in the Olkhon terrane (Fig. 13). It has a silicocarbonatite core with predominantly silicate mineralogy of clinopyroxene, phlogopite, scapolite, K-feldspar, titanite, and a opaque phase (looking brownish yellow on weathered surfaces) and only ≤ 15 vol. % silicates in the periphery. The thickest core part of the dyke has a banded structure produced by alternating zones rich and poor in silicate phases aligned with the dyke margins. It is obviously a body newly formed from a melt rather than being an entrapped fragment of skarn after the host amphibolite.

Clearly, neither granite nor any other felsic igneous lithologies, which are absent from the dyke vicinity, can be responsible for the skarn mineralization. In an overview on mantle- and crustal-derived igneous carbonatites, [Jin et al., 2024b] described three genetic models for melting and emplacement of carbonatitic magma in the crust (Fig. 14). One scenario (Fig. 14, a), similar to the model of [Lentz, 1999], implies low-degree partial melting of sedimentary carbonate material and intrusion of the melt at the upper crust levels; in this case, carbonatites are associated with skarn systems formed at the contact of felsic magma with carbonate sediment. In another scenario (Fig. 14, b), carbonate sediments melt in the lower crust by anatexis or high-grade regional metamorphism upon reactions with mantle-derived fluid-saturated melts. Finally, carbonatites can result from partial melting of recycled sedimentary carbonate rocks in subducting slabs (Fig. 14, c). However, the third model appears the least realistic as slabs commonly contain limited amounts of carbonate material. Subduction of seamounts with carbonate caps into the melting

region is also doubtful because they would plug the subduction zone and induce exhumation of the slab rocks. In this respect, only subduction of continental crust material with a carbonate component could be a workable scenario for the origin of crustal carbonatites.

The above models limit the formation of carbonatites to subduction zones. However, the mantle- and crustal-derived carbonatites were hypothesized to originate in intraplate (cratonic) and orogenic settings, respectively [Wang et al., 2023]. It seems not quite true at first sight given that crustal carbonatites were often reported from cratonic areas [Wan et al., 2008; Yang et al., 2012; Santos et al., 2013; Hegner et al., 2020; Wu et al., 2022; Wickramasinghe et al., 2024]. However, carbonatites in the latter case emplaced during tectonic events prior to final consolidation of cratonic blocks, or along rifting craton margins if carbonatitic magma formed long after the host cratons had consolidated (e.g. [Wang et al., 2023; Wickramasinghe et al., 2024]).

Data on crustal carbonatites from the Olkhon terrane are consistent with the scenario of anatectic melting of carbonate sediments and high-grade metamorphism. High-temperature metamorphism in the lower and middle crust is possible only in active tectonic settings, such as accretion, collision, rifting, or postcollisional extension [Sklyarov, 2001; Holder et al., 2019]. The Olkhon composite terrane represents the lower level of the Early Paleozoic collisional suture between the Siberian craton and the Barguzin microcontinent [Fedorovsky, Sklyarov, 2010]. In its early phase, the oblique craton-microcontinent convergence developed as a frontal collision leading to thrusting, with thickening and heating of the crust. At the late phase, strike-slip movements corresponding to transform faulting along plate boundaries [Khanchuk, Ivanov, 1999; Grebennikov, Khanchuk, 2021] became predominant. Mafic magma intruded the lower

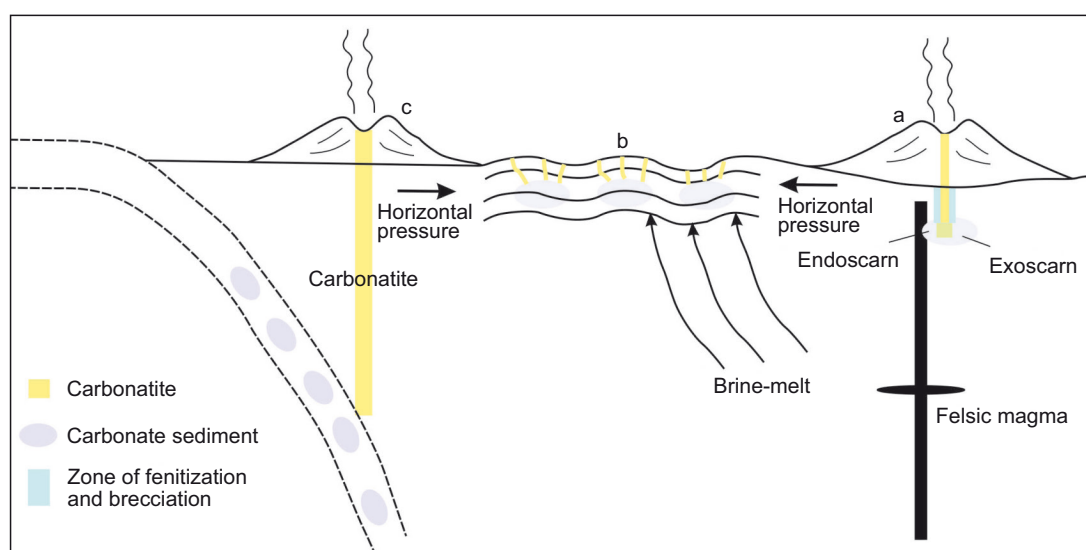


Fig. 14. Genetic diagram of crustal-derived carbonatite, after [Jin et al., 2024b].

a – primary sedimentary carbonate rocks are invaded by intermediate-acid magma while skarnification produces a large amount of water and heat that forms a small amount of carbonatite melt; b – some carbonatites are produced, as sporadic dykes, by anatexis or regional metamorphism at the lower-crust depths; c – carbonatites are produced by partial melting of recycled slab carbonate sediment.

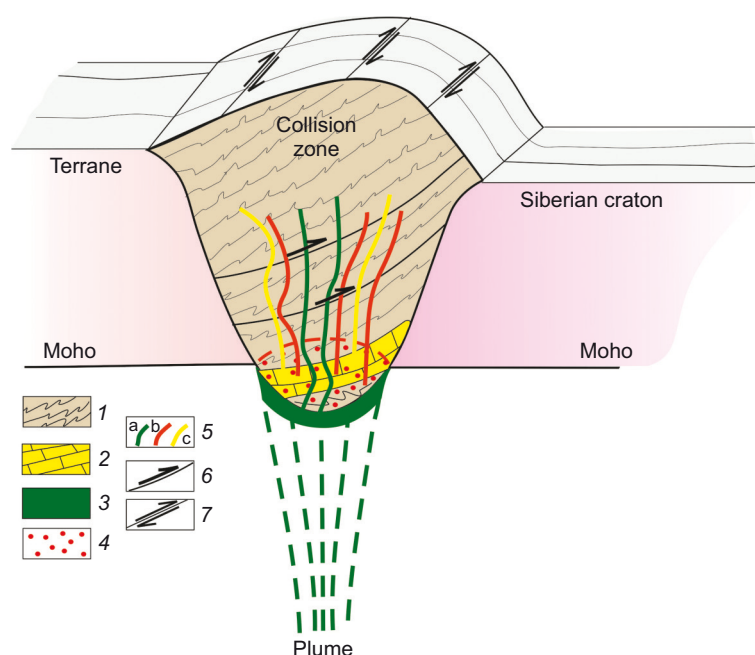


Fig. 15. Genetic diagram of crustal-derived carbonatite of the Olkhon terrane at the late collisional stage.

1 – silicate metamorphic complexes; 2 – marble; 3 – underplated mantle mafic melt; 4 – zone of partial melting of silicate and carbonate metamorphic rocks; 5 – dolerite (a), granite (b), and carbonatite (c) dykes; 6 – thrusts; 7 – strike-slip faults.

crust above a zone of underplated abnormally hot mantle and a deep zone of low shear velocities in the Sayan-Baikal fold area, which fits the hypothesis of a large low shear velocity province (LLSVP) existing in the region in the Late Precambrian to Mesozoic time span [Yarmolyuk et al., 2013]. In these conditions, the crust was heated up to temperatures maintaining the melting of silicate and carbonate material (Fig. 15). High-rate strike-slip faulting led to the formation of local pull-apart basins, where crustal granitic and carbonate melts, as well as batches of mantle-derived mafic magma, emplaced at the upper crust levels. Actually, this setting corresponds to postcollisional extension.

6. CONCLUSIONS

Proceeding from the summarized available data, we suggest the definition of crustal carbonatites as intrusive rocks containing >50 wt. % carbonates and ≤20 wt. % silicates, which crystallized from the carbonate melt derived as a result of partial melting of carbonate sedimentary rocks in the lower crust.

Crustal carbonatites are remarkable by

- 1) occurring as dykes, which are often misinterpreted as layers, protrusions, or hydrothermal veins in metamorphic complexes;
- 2) being limited to granulite-facies metamorphic complexes (though transport to the amphibolite-facies level is possible);
- 3) containing silicate minerals more common to metasomatic rocks due to the particular rock composition and carbonate-silicate interaction during magma cooling;
- 4) having isotope-geochemical signatures either corresponding to carbonate sediment or being intermediate between the latter and mantle-derived carbonatite;
- 5) emplacing during strike-slip movements (e.g. [Sklyarov et al., 2013, 2022]) or in settings of postcollisional extension (e.g. [Liu et al., 2006]).

Crustal carbonatites can form provided that

- primary carbonate sedimentary material is present in the lower crust;
- magma generation zone is sufficiently fluxed with H₂O-rich fluids;
- underplating (mafic mantle melts penetrating into the lower crust) maintains temperatures required for carbonate melting;
- tectonic activity in strike-slip, rifting, or postcollisional extension settings favors transport of carbonatitic melt to the upper crust levels.

7. ACKNOWLEDGEMENTS

We wish to thank O.A. Sklyarova and I.G. Barash for assistance in preparing figures. The manuscript profited from constructive criticism by T.B. Kolotilina and I.R. Prokopyev.

8. CONTRIBUTION OF THE AUTHORS

Both authors made an equivalent contribution to this article, read and approved the final manuscript.

9. DISCLOSURE

Both authors declare that they have no conflicts of interest relevant to this manuscript.

10. REFERENCES

- Anenburg M., Mavrogenes J.E., 2018. Carbonatitic Versus Hydrothermal Origin for Fluorapatite REE-Th Deposits: Experimental Study of REE Transport and Crustal "Antiskarn" Metasomatism. *American Journal of Sciences* 318 (3), 335–366. <https://doi.org/10.2475/03.2018.03>.
- Anenburg M., Walters J.B., 2024. Metasomatic Ijolite, Glimmerite, Silicocarbonatite, and Antiskarn Formation: Carbonatite and Silicate Phase Equilibria in the System Na₂O–CaO–K₂O–FeO–MgO–Al₂O₃–SiO₂–H₂O–O₂–CO₂. *Contributions*

to Mineralogy and Petrology 179, 40 <https://doi.org/10.1007/s00410-024-02109-0>.

Barnes C.G., Prestvik T., Sundvoll B., Surratt D., 2005. Pervasive Assimilation of Carbonate and Silicate Rocks in the Hortavaer Igneous Complex, North-Central Norway. *Lithos* 80 (1–4), 179–199. <https://doi.org/10.1016/j.lithos.2003.11.002>.

Bell K., 2005. Carbonatites. In: R.C. Selley, L.R.M. Cocks, I.R. Plimer (Eds), Vol. 3. *Encyclopedia of Geology*. Elsevier, p. 217–233.

Bell K., Tilton G.R., 2002. Probing the Mantle: The Story from Carbonatites. *Eos* 83 (25), 273–277. <https://doi.org/10.1029/2002EO000190>.

Brooker R.A., Kjarsgaard B.A., 2011. Silicate–Carbonate Liquid Immiscibility and Phase Relations in the System SiO_2 – Na_2O – Al_2O_3 – CaO – CO_2 at 0.1–2.5 GPa with Applications to Carbonatite Genesis. *Journal of Petrology* 52 (7–8), 1281–1305. <https://doi.org/10.1093/petrology/egq081>.

Carter L.B., Dasgupta R., 2016. Effect of Melt Composition on Crustal Carbonate Assimilation: Implications for the Transition from Calcite Consumption to Skarnification and Associated CO_2 Degassing. *Geochemistry, Geophysics, Geosystems* 17 (10), 3893–3916. <https://doi.org/10.1002/2016GC006444>.

Dolenec M., Serafimovski T., Daneu N., Dolenec T., Smuc N.R., Vrhovnik P., Lojen S., 2015. The Case of the Carbonatite-Like Dyke of the Madenska River Complex at the Kriva Lakavica Section in the Republic of Macedonia: Oxygen and Carbon Isotopic Constraints. *Turkish Journal of Earth Sciences* 24 (6), 627–639. <https://doi.org/10.3906/yer-1502-28>.

Doroshkevich A., Sklyarov E., Starikova A., Vasiliev V., Ripp G., Izbrodin I., Posokhov V., 2017. Stable Isotope (C, O, H) Characteristics and Genesis of the Tazheran Brucite Marbles and Skarns, Olkhon Region, Russia. *Mineralogy and Petrology* 111, 399–416. <https://doi.org/10.1007/s00710-016-0477-8>.

Durand C., Baumgartner L.P., Marquer D., 2015. Low Melting Temperature for Calcite at 1000 Bars on the Join CaCO_3 – H_2O – Some Geological Implications. *Terra Nova* 27 (5), 364–369. <https://doi.org/10.1111/ter.12168>.

Fanelli M.T., Cava N., Wyllie P.J., 1986. Calcite and Dolomite Without Portlandite at a New Eutectic in CaO – MgO – CO_2 – H_2O with Applications to Carbonatites. In: *Morphology and Phase Equilibria of Minerals. Proceedings of the 13th General Meeting of the International Mineralogical Association* (September 19–25, 1982, Varna). Bulgarian Academy of Science, Sofia, Bulgaria, p. 313–322.

Fedorovsky V.S., Sklyarov E.V., 2010. The Olkhon Geodynamic Proving Ground (Lake Baikal): High-Resolution Satellite Data and Geological Maps of New Generation. *Geodynamics & Tectonophysics* 1 (4), 331–418 (in Russian) [Федоровский В.С., Скляр Е.В. Ольхонский геодинамический полигон (Байкал): аэрокосмические данные высокого разрешения и геологические карты нового поколения // Геодинамика и тектонофизика. 2010. Т. 1. № 4. С. 331–418]. <https://doi.org/10.5800/GT-2010-1-4-0026>.

Fershtater G.B., Pushkarev E.V., 1988. Carbonate Rocks in the Kempirsai–Khabarny Complex, the South Urals. *Bulletin of the USSR Academy of Sciences. Geological Series* 12, 27–37 (in Russian) [Ферштатер Г.Б., Пушкирев Е.В. Карбонатные породы в офиолитовом Кемпирсайско-Хабарнинском комплексе (Южный Урал) // Известия АН СССР. Серия геологическая. 1988. № 12. С. 27–37].

Floess D., Baumgartner L.P., Vonlanthen P., 2015. An Observational and Thermodynamic Investigation of Carbonate Partial Melting. *Earth and Planetary Science Letters* 409, 147–156. <https://doi.org/10.1016/j.epsl.2014.10.031>.

Gaeta M., Di Rocco T., Freda C., 2009. Carbonate Assimilation in Open Magmatic Systems: The Role of Melt-Bearing Skarns and Cumulate-Forming Processes. *Journal of Petrology* 50 (1), 361–385. <https://doi.org/10.1093/petrology/egp002>.

Ganino C., Arndt N.T., Chauvel C., Jean A., Athurion C., 2013. Melting of Carbonate Wall Rocks and Formation of the Heterogeneous Aureole of the Panzhihua Intrusion, China. *Geoscience Frontiers* 4 (5), 535–546. <https://doi.org/10.1016/j.gsf.2013.01.012>.

Grebennikov A.V., Khanchuk A.I., 2021. Pacific-Type Transform and Convergent Margins: Igneous Rocks, Geochemical Contrasts and Discriminant Diagrams. *International Geology Review* 63 (5), 601–629. <https://doi.org/10.1080/00206814.2020.1848646>.

Hegner E., Rajesh S., Willbold M., Müller D., Joachimski M., Hofmann M., Linnemann U., Zieger J., Pradeepkumar A.P., 2020. Sediment-Derived Origin of the Putative Munnar Carbonatite, South India. *Journal of Asian Earth Sciences* 200, 104432. <https://doi.org/10.1016/j.jseaes.2020.104432>.

Holder R.M., Viete D.R., Brown M., Johnson T.E., 2019. Metamorphism and the Evolution of Plate Tectonics. *Nature* 572, 378–381. <https://doi.org/10.1038/s41586-019-1462-2>.

Humphreys-Williams E.R., Zahirovic S., 2021. Carbonatites and Global Tectonics. *Elements* 17 (5), 339–344. <https://doi.org/10.2138/gselements.17.5.339>.

Iacono Marziano G., Gaillard F., Pichavant M., 2008. Limestone Assimilation by Basaltic Magmas: An Experimental Re-Assessment and Application to Italian Volcanoes. *Contributions to Mineralogy and Petrology* 155, 719–738. <https://doi.org/10.1007/s00410-007-0267-8>.

Jin C., Cheng Z., Zhang Z., Hou T., Xu L., 2024a. Petrogenesis of the Wushi Carbonatites in the Northwestern Tarim Basin: Implications to Deep Carbon Recycling. *Lithos* 464–465, 107448. <https://doi.org/10.1016/j.lithos.2023.107448>.

Jin C., Zhang Z., Cheng Z., 2024b. Carbonatite and Related Mineralization: An Overview. In: R. Pandey, A. Pandey, L. Krmíček, C. Cicciniello, D. Müller (Eds), *Alkaline Rocks: Economic and Geodynamic Significance Through Time*. Geological Society of London Special Publications 551. <https://doi.org/10.1144/SP551-2024-51>.

Keller J., Hoefs J., 1995. Stable Isotope Characteristics of Recent Natrocarbonatites from Oldoinyo Lengai. In: K. Bell, J. Keller (Eds), *Carbonatite Volcanism: Oldoinyo Lengai and*

the Petrogenesis of Natrocarbonatites. Springer, Berlin, Heidelberg, p. 113–123. https://doi.org/10.1007/978-3-642-79182-6_9.

Khanchuk A.I., Ivanov V.V., 1999. Meso-Cenozoic Geodynamic Settings and Gold Mineralization of the Russian Far East. *Russian Geology and Geophysics* 40 (11), 1607–1617.

Korzhinskii D.S., 1970. *Theory of Metasomatic Zoning*. Clarendon Press, Oxford, 162 p.

Le Bas M.J., Babbat M.A.O., Taylor R.N., Milton J.A., Windley B.F., Evins P.M., 2004. The Carbonatite-Marble Dykes of Abyan Province, Yemen Republic: The Mixing of Mantle and Crustal Carbonate Materials Revealed by Isotope and Trace Element Analysis. *Mineralogy and Petrology* 82, 105–135. <https://doi.org/10.1007/s00710-004-0056-2>.

Le Maitre R.W. (Ed.), 2002. *Igneous Rocks: A Classification and Glossary of Terms*. Cambridge University Press, Cambridge, 251 p. <https://doi.org/10.1017/CBO9780511535581>.

Lentz D.R., 1998. Late-Tectonic U-Th-Mo-REE Skarn and Carbonatitic Vein-Dyke Systems in the Southwestern Grenville Province: A Pegmatite-Related Pneumatolytic Model Linked to Marble Melting. In: D.R. Lentz (Ed.), *Mineralized Intrusion-Related Skarn Systems*. Vol. 26. Mineralogical Association of Canada, Ottawa, p. 519–657.

Lentz D.R., 1999. Carbonatite Genesis: A Reexamination of the Role of Intrusion-Related Pneumatolytic Skarn Processes in Limestone Melting. *Geology* 27 (4), 335–338. [https://doi.org/10.1130/0091-7613\(1999\)027%3C0335:CGAROT%3E2.3.CO;2](https://doi.org/10.1130/0091-7613(1999)027%3C0335:CGAROT%3E2.3.CO;2).

Liu Y., Berner Z., Massonne H.-J., Zhong D., 2006. Carbonatite-Like Dykes from the Eastern Himalayan Syntaxis: Geochemical, Isotopic, and Petrogenetic Evidence for Melting of Metasedimentary Carbonate Rocks Within the Orogenic Crust. *Journal of Asian Earth Sciences* 26 (1), 105–120. <https://doi.org/10.1016/j.jseaes.2004.10.003>.

Meinert L.D., 1992. Skarns and Skarn Deposits. *Geoscience Canada* 19 (4), 145–162.

Mitchell R.H., 2005. Carbonatites and Carbonatites and Carbonatites. *The Canadian Mineralogist* 43 (6), 2049–2068. <https://doi.org/10.2113/gscanmin.43.6.2049>.

Mollo S., Gaeta M., Freda C., Di Rocco T., Misiti V., Scarlato P., 2010. Carbonate Assimilation in Magmas: A Reappraisal Based on Experimental Petrology. *Lithos* 114 (3–4), 503–514.

Proskurnin V.F., Petrov O.V., Gavrish A.V., Paderin P.G., Mozoleva I.N., Petrushkov B.S., Bagaeva A.A., 2010. The Early Mesozoic Carbonatite Zone of Taimyr Peninsula. *Lithosphere* 3, 95–102 (in Russian) [Проскурнин В.Ф., Петров О.В., Гавриш А.В., Падерин П.Г., Мозолева И.Н., Петрушков Б.С., Багаева А.А. Раннемезозойский пояс карбонатитов полуострова Таймыр // Литосфера. 2010. № 3. С. 95–102].

Roberts D., Zwaan K.B., 2007. Marble Dykes Emanating from Marble Layers in an Amphibolite-Facies, Multiply-Deformed Carbonate Succession, Troms, Northern Norway. *Geological Magazine* 144 (5), 883–888. <https://doi.org/10.1017/S0016756807003810>.

Santos R.V., dos Santos E.J., de Souza Neto J.A., Carmo L.C.M., Sial A.N., Mancini L.H., de Lira Santos L.C.M., do Nascimento G.H., Mendes L.U.S., Anastácio E.M.F., 2013. Isotope Geochemistry of Paleoproterozoic Metacarbonates from Itatuba, Borborema Province, Northeastern Brazil: Evidence of Marble Melting Within a Collisional Suture. *Gondwana Research* 23 (1), 380–389. <https://doi.org/10.1016/j.gr.2012.04.010>.

Sklyarov E.V. (Ed.), 2001. *Metamorphism and Tectonics*. Textbook. Internet Engineering, Moscow, 216 p. (in Russian) [Метаморфизм и тектоника: Учебное пособие / Ред. Е.В. Скляров. М.: Интернет Инжиниринг, 2001. 216 с.].

Sklyarov E.V., Fedorovsky V.S., Kotov A.B., Lavrenchuk A.V., Mazukabzov A.M., Levitsky V.I., Sal'nikova E.B., Starikova A.E., Yakovleva S.Z., Anisimova I.V., Fedoseenko A.M., 2009. Carbonatites in Collisional Settings and Pseudo-Carbonatites of the Early Paleozoic Ol'khon Collisional System. *Russian Geology and Geophysics* 50 (12), 1091–1106. <https://doi.org/10.1016/j.rgg.2009.11.008>.

Sklyarov E.V., Fedorovsky V.S., Kotov A.B., Lavrenchuk A.V., Mazukabzov A.M., Starikova A.E., 2013. Carbonate and Silicate-Carbonate Injection Complexes in Collision Systems: The West Baikal Region as an Example. *Geotectonics* 47 (3), 180–196. <https://doi.org/10.1134/S0016852113020064>.

Sklyarov E.V., Lavrenchuk A.V., Doroshkevich A.G., Starikova A.E., Kanakin S.V., 2021. Pyroxenite as a Product of Mafic-Carbonate Melt Interaction (Tazheran Massif, West Baikal Area, Russia). *Minerals* 11 (6), 654. <https://doi.org/10.3390/min11060654>.

Sklyarov E.V., Lavrenchuk A.V., Fedorovsky V.S., Gladkochub D.P., Donskaya T.V., Kotov A.B., Mazukabzov A.M., Starikova A.E., 2020. Regional, Contact Metamorphism, and Autometamorphism of the Olkhon Terrane (West Baikal Area). *Petrology* 28, 47–61. <https://doi.org/10.1134/S0869591120010051>.

Sklyarov E.V., Lavrenchuk A.V., Mazukabzov A.M., 2022. Marble Dikes in the Olkhon Composite Terrane (West Baikal Area). *Geodynamics & Tectonophysics* 13 (5), 0667 (in Russian) [Скляров Е.В., Лавренчук А.В., Мазукабзов А.М. Дайки мраморов и кальцифиров Ольхонского композитного террейна (Западное Прибайкалье, Россия). Геодинамика и тектонофизика. 2022. Т. 13. № 5. 0667]. <https://doi.org/10.5800/GT-2022-13-5-0667>.

Sklyarov E.V., Lavrenchuk A.V., Semenova D.V., 2024. Assimilation of Carbonates by Mafic Magma: Fassaitte Gabbro of the Olkhon Terrane (Western Baikal Region). *Doklady Earth Sciences* 519, 1860–1867. <https://doi.org/10.1134/S1028334X24603055>.

Su B.-X., Wang S.-Y., Dharmapriya P.L., Wang J., Malaviarachchi S.P.K., Yang K.-F., Fan H.-R., 2024a. Crustal Anatectic Origin of the Pegmatitic Carbonate Rocks in the Proterozoic Highland Complex, Sri Lanka. *Contribution to Mineralogy and Petrology* 179, 96. <https://doi.org/10.1007/s00410-024-02178-1>.

Su B.-X., Wang S.-Y., Wang J., Fan H.-R., 2024b. Crustal-Derived Versus Mantle-Derived Carbonatites. *Lithos* 488–489, 107826. <https://doi.org/10.1016/j.lithos.2024.107826>.

Vuorinen J.H., Skelton A.D.L., 2004. Origin of Silicate Minerals in Carbonatites from Alnö Island, Sweden: Magmatic Crystallization or Wall Rock Assimilation? *Terra Nova* 16 (4), 210–215. <https://doi.org/10.1111/j.1365-3121.2004.00557.x>.

Wan Y., Liu D., Xu Z., Dong C., Wang Z., Zhou H., Yang Z., Liu Z., Wu J., 2008. Paleoproterozoic Crustally Derived Carbonate-Rich Magmatic Rocks from the Daqinshan Area, North China Craton: Geological, Petrographical, Geochronological and Geochemical (Hf, Nd, O and C) Evidence. *American Journal of Science* 308 (3), 351–378. <https://doi.org/10.2475/03.2008.07>.

Wang Ch., Foley S.F., Liu Y., Wang Y., Xu Y.-G., 2023. Origin of Carbonate Melts in Orogenic Belts by Anatexis of Downthrust Carbonate Sediments. *Earth and Planetary Science Letters* 619, 18303. <https://doi.org/10.1016/j.epsl.2023.118303>.

Warr L.N., 2021. IMA–CNMNC Approved Mineral Symbols. *Mineralogical Magazine* 85 (3), 291–320. <https://doi.org/10.1180/mgm.2021.43>.

Watkinson D.H., Wyllie P.J., 1971. Experimental Study of the Composition Join NaAlSiO_4 – CaCO_3 – H_2O and the Genesis of Alkaline Rock–Carbonatite Complexes. *Journal of Petrology* 12 (2), 357–378. <https://doi.org/10.1093/petrology/12.2.357>.

Wickramasinghe W.A.G.K., Madugalla T.B.N.S., Athurupana B., Zhao L., Zhai M., Li X., Pitawala H.M.T.G.A., 2024.

An Unusual Occurrence of Carbonatites Derived from the Crust in the UHT Granulite Facies Metamorphic Terrain of Sri Lanka. *Precambrian Researches* 450, 107502. <https://doi.org/10.1016/j.precamres.2024.107502>.

Wu H., Zhu W., Ge R., 2022. Evidence for Carbonatite Derived from the Earth's Crust: The Late Paleoproterozoic Carbonate-Rich Magmatic Rocks in the Southeast Tarim Craton, Northwest China. *Precambrian Research* 369 (5), 106425. <https://doi.org/10.1016/j.precamres.2021.106425>.

Wyllie P.J., Tuttle O.F., 1960. The System CaO – CO_2 – H_2O and the Origin of Carbonatites. *Journal of Petrology* 1 (1), 1–46. <https://doi.org/10.1093/petrology/1.1.1>.

Yang J.Q., Wan Y.S., Liu Y.S., Xin H.T., Zhang S.R., Li M.Z., 2012. Discovery of Paleoproterozoic Crustally Derived Carbonatite in the Northern Altyn Tagh. *Earth Science* 37 (5), 929–936. DOI: 10.3799/dqkx.2012.101.

Yarmolyuk V.V., Kuzmin M.I., Vorontsov A.A., 2013. West Pacific-Type Convergent Boundaries and Their Role in the Formation of the Central Asian Fold Belt. *Russian Geology and Geophysics* 54 (12), 1427–1441. <https://doi.org/10.1016/j.rgg.2013.10.012>.

Yaxley G.M., Brey G.P., 2004. Phase Relations of Carbonate-Bearing Eclogite Assemblages from 2.5 to 5.5 GPa: Implications for Petrogenesis of Carbonatites. *Contributions to Mineralogy and Petrology* 146, 606–619. <https://doi.org/10.1007/s00410-003-0517-3>.